GENERAL PHYSICS

I. MOLECULAR BEAMS

Prof. J. R. Zacharias
Prof. J. G. King
Prof. C. L. Searle
Prof. K. W. Billman
Prof. E. F. Taylor

R. S. Badessa
J. F. Brenner
R. Golub
G. L. Guttrich
W. D. Johnston, Jr.

S. G. Kukolich
F. J. O'Brien
R. D. Posner
C. O. Thornburg, Jr.
L. H. Veneklasen

RESEARCH OBJECTIVES

Three kinds of research are carried on in the Molecular Beams group.

1. High-precision studies of atomic and molecular radiofrequency spectra.

2. Experiments directed toward establishing precise frequencies generated by atomic clocks of proved independence from external influence, and the intercomparison of these frequencies.

3. Experiments such as

(a) measurement of the velocity of light in terms of atomic standards,

(b) search for a charge carried by molecules, both by gas efflux and beam deflection methods,

(c) study of atomic beams from liquid helium,

(d) an experiment on an aspect of continuous creation.

These experiments are described in more detail below.

J. R. Zacharias, J. G. King, C. L. Searle

1. RF Spectra

The most recent examples of investigations of RF spectra are the rotational spectrum of HF and the hyperfine structure of the stable bromine isotropes. A study of certain NH_3 lines to a resolution approximately 10 times that hitherto attained is now under way as part of an effort to produce a molecular frequency standard. Results of measurements of the magnetic hfs in the 3-2 line of NH_3 were reported in Quarterly Progress Report No. 74 (pages 4-7).

J. G. King, S. G. Kukolich, J. R. Zacharias

2. Molecular Clocks

Development of clocks depending on purely electric interactions for comparison with Cs and H atomic clocks is in progress. A promising device is the two-cavity NH_3 maser, which overcomes some of the inherent difficulties of the single-cavity maser. The origin of certain frequency dependences is being investigated.

S. G. Kukolich

3. Atomic Clocks

A Cs clock of moderate length which incorporates several novel features is being developed. Every effort will be made to control and minimize the known sources of frequency instability. It should be possible with this design to achieve stability and resetability in the 10^{-13} range.

C. O. Thornburg, Jr.

4. Intercomparison of Clocks

The electronic techniques for generating frequencies and locking them to atomic resonances have been extensively improved. Recent experience with frequency impulse modulation shows that it not only obviates the bad effects of modulation distortion upon locking to the atomic resonance but also makes it possible to eliminate the effects of differences in phase of the RF cavities of a frequency standard with separated oscillating fields. Use of this method of modulation has resulted in improvement by a factor of 10 in the performance of commercial atomic clocks, to the point where the effects of temperature and magnetic field are now dominant.

As part of the program of intercomparison, methods for computer calculation of the power spectrum of the phase fluctuations between frequency standards have been developed and tried during the past year and appear to be extremely promising.

C. L. Searle, R. S. Badessa, R. D. Posner

5. Decelerator for Molecules

An apparatus is being constructed to make use of nonuniform pulsed electric fields for slowing down molecules to smaller velocities than have hitherto been observed. The design of the apparatus has been placed on a firmer foundation during the past year, and construction has progressed at a satisfactory rate. Such molecules will yield narrow spectral lines, and make new studies of molecular collisions possible.

R. Golub, G. Guttrich

6. Velocity of Light

By investigating the resonances of an adjustable precision nicrowave cavity for both light and microwaves, one can, with suitable corrections, establish the ratio of the two wavelengths that are used; this can be interpreted either as the ratio of certain fundamental constant or (through the usual standards) as the velocity of light. The results of other investigations have yielded results to approximately 10^{-6}, and we expect to achieve 10^{-8}

M. A. Yaffee, C. L. Searle, J. R. Zacharias

7. Neutrality of Atoms

Whether neutral atoms are really neutral or carry a slight charge that is due, perhaps, to a difference in the charge of the electron and proton is a question of fundamental importance. Two experiments designed to set upper limits on such charge unbalances are being performed. In one, a large volume of deionized gas is allowed to emerge from a container. Limits around 2×10^{-20} fundamental charge per atom can be placed on such gases as H_2, D_2 and He. A limit lower by approximately a factor of 10 would be attainable were it not for some still unexplained effects that are now being investigated. In another experiment a beam of Cs atoms is deflected by large modulated electric field — the limit on the charge carried by a Cs atom determined in the preliminary experiments is approximately 20 times better than previous work reported by others.

K. W. Billman, J. G. King

8. Helium Beams

Apparatus has been designed and is now under construction for the purpose of observing helium beams directly emitted from liquid He^3 and He^4 surfaces below 4°K.

We plan first to study the fluctuations and velocity distribution in the beam from which the temperature can be determined for comparison with the results of other methods. The results of this experiment are definitely predicted by theory, but an unusual liquid such as He may exhibit anomalous behavior.

W. D. Johnston, Jr., J. F. Brenner

9. Mercury Boiling Experiment

In this experiment we seek to place an upper limit on the appearance of hydrogen in mercury. The apparatus is essentially a mercury still with a scanning mass spectrometer. The object of the experiment is to test a remotely conceivable density-dependent continuous creation hypothesis.

E. F. Taylor, J. G. King

A. TWO-CAVITY MASER MOLECULAR RESONANCE CLOCK

The physical construction and electronic system for the NH_3 maser with separated oscillating fields have been described previously.[1-3] A diagram of the present system is shown in Fig. I-1. The frequency stability and resetability of this system has been measured by using as a reference standard the cesium clocks built by V. J. Bates and R. S. Badessa.[4]
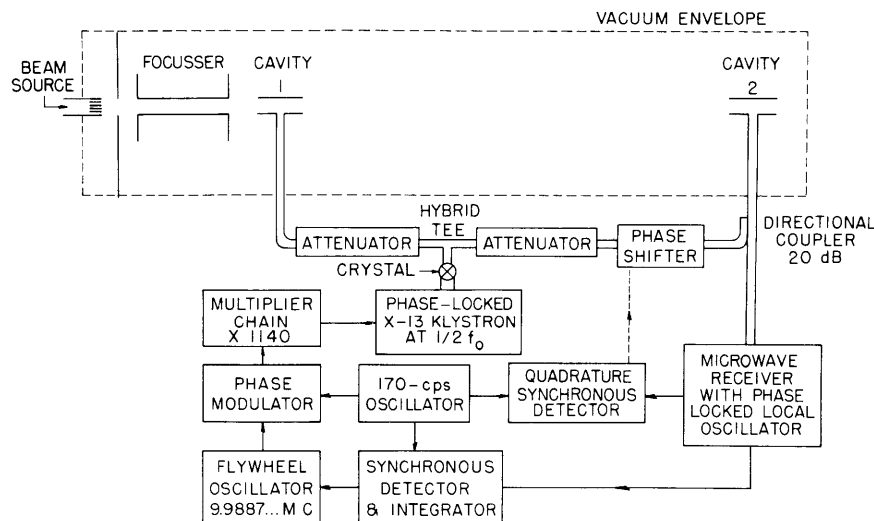

Fig. I-1. The two-cavity maser.

When cavity temperatures, stimulating power level and cavity phase difference are carefully stabilized, the observed rms frequency deviation is 3×10^{-11} for a 12-hour period. The rms deviation for runs on different days is typically 1×10^{-10}, when the stimulating power and cavity temperature are reset. But when gross changes were made

in the electronics or the microwave cavities, changes as large as 1×10^{-9} were observed. It is believed that these large changes resulted from the removal of shifts associated with an asymmetric stimulating signal spectrum or stray RF fields.

The shift of resonance frequency with stimulating power has now been reduced to -2 cps/db by using new cavities. The new cylindrical TM_{010}-mode cavities have a section, 1.5 cm long with an inside diameter $\lambda_o/2 \approx 0.5$ cm, attached to each end. These sections are well below the cutoff diameter, and considerably reduce the leakage of microwave power out of the ends of the cavities.

It is believed that the main contribution to the frequency deviations of this system are the power shift, the presence of small electric fields in the drift region, and fluctuations in the cavity temperature. The power shift appears to be the most important contribution, and there is definite correlation between the power shift and the quadrature error signal. We shall show that the existence of different power levels in the two cavities is not responsible for the power shift. The dependence of frequency on cavity temperature[1] is approximately 1 cps/°C. Electric fields in the drift region produce a quadratic frequency shift of approximately 12 cps for a 1 volt/cm field. It should be possible to reduce these shifts successfully so that the long-term stability and resetability will be 10^{-11}.

1. Theory of the Two-Cavity Maser

An arbitrary state of the two-level ammonia inversion system may by represented as a linear combination of the upper- and lower-state eigenfunctions u_a and u_b ($\psi = au_a + bu_b$, where a and b are complex and subject to the condition $a^*a + b^*b = 1$). It is convenient to use the spinor representation $\psi = \begin{pmatrix} a \\ b \end{pmatrix}$, since the resulting Schrödinger equation will be the same as that for spin $\frac{1}{2}$ particles in a magnetic field.[5] Then the Hamiltonian for this system when no external fields are present is $\mathcal{3C}_o = \frac{\hbar\omega_o}{2} \sigma_z$ and $\psi^* \mathcal{3C}_o \psi = \frac{\hbar\omega_o}{2} (a^*a - b^*b)$, where $\hbar\omega_o$ is the energy separation between the inversion levels, and σ_z is a Pauli spin matrix. An applied rf field provides a perturbation of the form

$$V_I = \begin{pmatrix} 0 & \frac{\hbar\omega_1}{2} e^{i\omega t} \\ \frac{\hbar\omega_1}{2} e^{-i\omega t} & 0 \end{pmatrix} .$$

and the Schrödinger equation i $\frac{\partial}{\partial t} \psi = \mathcal{3C}\psi$ is

$$i\frac{\partial}{\partial t}\begin{pmatrix} a \\ b \end{pmatrix} = \begin{pmatrix} \dfrac{\omega_o}{2} & \dfrac{\omega_1}{2}e^{i\omega t} \\ \dfrac{\omega_1}{2}e^{-i\omega t} & -\dfrac{\omega_o}{2} \end{pmatrix}\begin{pmatrix} a \\ b \end{pmatrix},$$

where $\hbar\omega_1 = \mu_{ab}\mathscr{E}_o$, μ_{ab} is the dipole matrix element between the upper and lower states, and $\mathscr{E}_o$ is the magnitude of the rf field. $(\mu_{aa} = \mu_{bb} = 0)$. If we make the substitution

$$\begin{pmatrix} a \\ b \end{pmatrix} = \begin{pmatrix} a' & e^{i\frac{\omega}{2}t} \\ b' & e^{-i\frac{\omega}{2}t} \end{pmatrix},$$

the Schrödinger equation becomes

$$i\frac{\partial}{\partial t}\begin{pmatrix} a' \\ b' \end{pmatrix} = \begin{pmatrix} \dfrac{\omega_o - \omega}{2} & \dfrac{\omega_1}{2} \\ \dfrac{\omega_1}{2} & -\left(\dfrac{\omega_o - \omega}{2}\right) \end{pmatrix}\begin{pmatrix} a' \\ b' \end{pmatrix}.$$

This equation has been solved by Abragam[6]:

$$\begin{pmatrix} a'(t) \\ b'(t) \end{pmatrix} = u\begin{pmatrix} a(0) \\ b(0) \end{pmatrix} = \begin{pmatrix} \cos at + i\left(\dfrac{\omega_o - \omega}{2a}\right)\sin at, & i\dfrac{\omega_1}{2a}\sin at \\ i\left(\dfrac{\omega_1}{2a}\right)\sin at, & \cos at - i\left(\dfrac{\omega_o - \omega}{2a}\right)\sin at \end{pmatrix}\begin{pmatrix} a(0) \\ b(0) \end{pmatrix},$$

where $a^2 = \dfrac{\omega_o - \omega}{2}^2 + \dfrac{\omega_1}{2}^2$. The initial state selected by the focusser is $\psi_o = \begin{pmatrix} 1 \\ 0 \end{pmatrix}$. The state produced by an rf field that is on for a time τ is

$$\begin{pmatrix} a' \\ b' \end{pmatrix} = \begin{pmatrix} \cos a\tau + i\left(\dfrac{\omega_o - \omega}{2a}\right)\sin a\tau & \dfrac{i\omega_1}{2a}\sin a\tau \\ i\dfrac{\omega_1}{2a}\sin a\tau & \cos a\tau + i\dfrac{\omega_o - \omega}{2a}\sin a\tau \end{pmatrix}\begin{pmatrix} a(0) \\ b(0) \end{pmatrix}.$$

For the first cavity we define

$$\cos a\tau + i\left(\frac{\omega_o - \omega}{2a}\right)\sin a\tau = \beta_I, \qquad i\frac{\omega_1}{2a}\sin a\tau = \gamma_I.$$

$$\begin{pmatrix} a' \\ b' \end{pmatrix}_I = \Omega_I \begin{pmatrix} a(o) \\ b(o) \end{pmatrix} = \begin{pmatrix} \beta_I & \gamma_I \\ \gamma_I & \beta_I^* \end{pmatrix} \begin{pmatrix} 1 \\ 0 \end{pmatrix} = \begin{pmatrix} \beta_I \\ \gamma_I \end{pmatrix}.$$

In the two-cavity maser the level of ω_1 in the first cavity is adjusted so that $\omega_1 \approx \frac{\pi}{2\tau}$, where τ is the average time that the molecules spend in the first cavity. The resonance width, $\Delta\omega$, for the validity of this condition is approximately $\Delta\omega = \omega_1 = \frac{\pi}{2\tau}$. This produces a transition probability $b^*b = \frac{1}{2}$, and the wave function

$$\begin{pmatrix} a' \\ b' \end{pmatrix}_I = \frac{1}{\sqrt{2}} \begin{pmatrix} 1 \\ i \end{pmatrix} \quad so \quad \begin{pmatrix} a \\ b \end{pmatrix}_I = \frac{1}{\sqrt{2}} \begin{pmatrix} e^{\frac{i\omega_0}{2}t} \\ i\, e^{-\frac{i\omega_0}{2}t} \end{pmatrix}.$$

The average energy is

$$E_I = \frac{\hbar\omega_0}{2} \langle \sigma_z \rangle = \frac{\hbar\omega_0}{2}(a^*a - b^*b) = 0,$$

and there is an oscillating polarization

$$P = P_0 \langle \sigma_x \rangle = P_0(a^*b + b^*a) = -P_0 \sin\omega_0 t.$$

In the region between the cavities the rf fields are very small, and the matrix is

$$\Omega_{II} = \begin{pmatrix} e^{i\left(\frac{\omega_0 - \omega}{2}\right)T} & 0 \\ 0 & e^{-i\left(\frac{\omega_0 - \omega}{2}\right)T} \end{pmatrix},$$

where T is the time spent by molecules in the region between the cavities.

The final wave function, after the molecules have passed through the two-cavity system, is

$$\begin{pmatrix} a' \\ b' \end{pmatrix}_{III} = \Omega_{III}\Omega_{II}\Omega_I \begin{pmatrix} a(0) \\ b(0) \end{pmatrix}.$$

where Ω_I represents the effect of the first cavity; Ω_{II}, the field-free drift space between the cavities, and Ω_{III}, the effect of the second cavity.

$$\Omega_{III} = \begin{pmatrix} \beta_{III} & \gamma_{III} \\ \gamma_{III} & \beta_{III}^* \end{pmatrix} = \begin{pmatrix} \cos \alpha'\tau + i\left(\frac{\omega_0-\omega}{2\alpha'}\right)\sin \alpha'\tau, & \left(i\frac{\omega_1'}{2\alpha'}\right)\sin \alpha'\tau \\ i\left(\frac{\omega_1'}{2\alpha'}\right)\sin \alpha\tau, & \cos \alpha'\tau - i\left(\frac{\omega_0-\omega}{2\alpha'}\right)\sin \alpha'\tau \end{pmatrix}$$

which is the same form as Ω_I, but the field strength ω_1 may be different. For the initial condition $\psi_0 = \begin{pmatrix} 1 \\ 0 \end{pmatrix}$,

$$\begin{pmatrix} a' \\ b' \end{pmatrix}_{III} = \begin{pmatrix} \beta_{III} & \gamma_{III} \\ \gamma_{III} & \beta_{III}^* \end{pmatrix}\begin{pmatrix} e^{i\left(\frac{\omega_0-\omega}{2}\right)T} & 0 \\ 0 & e^{-i\left(\frac{\omega_0-\omega}{2}\right)T} \end{pmatrix}\begin{pmatrix} \beta_I & \gamma_I \\ \gamma_I & \beta_I^* \end{pmatrix}\begin{pmatrix} 1 \\ 0 \end{pmatrix}$$

$$\begin{pmatrix} a' \\ b' \end{pmatrix}_{III} = \begin{pmatrix} \beta_{III}\beta_I\, e^{i\left(\frac{\omega_0-\omega}{2}\right)T} + \gamma_{III}\gamma_I\, e^{-i\left(\frac{\omega_0-\omega}{2}\right)T} \\ \gamma_{III}\beta_I\, e^{i\left(\frac{\omega_0-\omega}{2}\right)T} + \beta_{III}^*\gamma_I\, e^{-\left(\frac{\omega_0-\omega}{2}\right)T} \end{pmatrix}$$

the total transition probability for the two cavity system is

$$(b^*b)_{III} = (b'^*b')_{III} = \left(\frac{a^*a+b^*b}{2}\right) - \left(\frac{a^*a-b^*b}{2}\right) = \frac{1}{2} - \frac{1}{2}\langle \sigma_z \rangle_{III}$$

$$b' = \cos\left(\frac{\omega_0-\omega}{2}\right)T(\gamma_{III}\beta_I + \beta_{III}^*\gamma_I) + i\sin\left(\frac{\omega_0-\omega}{2}\right)T(\gamma_{III}\beta_I - \beta_{III}^*\gamma_I)$$

$$(b^*b)_{III} = -\cos^2\left(\frac{\omega_0-\omega}{2}\right)T\,[(\gamma_{III}\beta_I^* + \beta_{III}\gamma_I)(\bar\gamma_{III}\beta_I + \beta_{III}^*\gamma_I)]$$

$$-\sin^2\left(\frac{\omega_0-\omega}{2}\right)T[(\gamma_{III}\beta_I^* + \beta_{III}\gamma_I)(\gamma_{III}\beta_I - \beta_{III}^*\gamma_I)]$$

$$- i\cos\left(\frac{\omega_0-\omega}{2}\right)T\,\sin\left(\frac{\omega_0-\omega}{2}\right)T[2\gamma_I\gamma_{III}(\beta_I^*\beta_{III} - \beta_I\beta_{III}^*)].$$

(Note that the minus sign occurs because the γ are pure imaginary.)

The first two terms are both symmetric functions of $(\omega_0 - \omega)$, and the last term is the product of two antisymmetric functions and thus is also symmetric. This means that the resonance peak at ω_0 will not be shifted if the two rf fields have different strengths $(\omega_1 \neq \omega_1'$ and $\gamma_I \neq \gamma_{III})$, since the resonance pattern will be modified in a symmetrical way. This problem has also been considered by Ramsey.[7]

For conditions near the center of the resonance $\left(\omega_0 - \omega < \frac{1}{T}\right)$

$$\beta_I \cong \cos\frac{\omega_1 T}{2} \qquad \gamma_I \cong i \sin\frac{\omega_1 T}{2}$$

$$\beta_{III} \cong \cos\frac{\omega_1' T}{2} \qquad \gamma_{III} \cong i \sin\frac{\omega_1' T}{2},$$

and the last term in $(b^* b)_{III}$ vanishes. If the rf field strengths are equal, the second term vanishes also, and

$$(b^* b)_{III} = \sin^2 \omega_1 T \cos^2\left(\frac{\omega_0 - \omega}{2}\right) T$$

(see Ramsey[8]).

For the two-cavity maser, conditions in the first cavity are nearly such that $\beta_I = \frac{1}{\sqrt{2}}$, $\gamma_I = \frac{1}{\sqrt{2}}$, and the average energy just before the second cavity is

$$E_{II} = \frac{\hbar\omega_0}{2} \left\langle \sigma_z \right\rangle_{II} = 0.$$

After the second cavity, the average energy is

$$E_{III} = \frac{\hbar\omega_0}{2} \left\langle \sigma_z \right\rangle_{III} = \hbar\omega_0 \left[\frac{1}{2} - (b^* b)_{III} \right].$$

If there are n molecules per second, the power delivered to the second cavity is

$$W = n \ (E_{II} - E_{III})$$

$$W = n \ \hbar \omega_0 \left[(b^* b)_{III} - \frac{1}{2} \right].$$

and the resonance behavior will be determined by $(b^* b)_{III}$. $[(b^* b)_{III} = P_{ab}]$. For these conditions,

$$(b^*b)_{III} \cong \frac{1}{2} + \frac{1}{2} \sin\left(\frac{\omega_1' \tau}{2}\right) \cos\left(\frac{\omega_1' \tau}{2}\right) \left[\cos^2\left(\frac{\omega_0 - \omega}{2}\right)T - \sin^2\left(\frac{\omega_0 - \omega}{2}\right)T\right]$$

$$(b^*b)_{III} \cong \frac{1}{2} + \frac{1}{2} \sin(\omega_1' \tau)[\cos(\omega_0 - \omega)T].$$

The velocity distribution in the beam will provide a distribution of transit times T, and reduce the amplitude of other maxima relative to the central maximum at $(\omega_0 - \omega) = 0$.[8] The factor $\sin(\omega_1' \tau)$ reduces the resonance signal if the rf field is less than the optimum value $\left(\omega_1 \tau = \frac{\pi}{2}\right)$.

S. G. Kukolich

References

1. S. G. Kukolich, Quarterly Progress Report No. 72, Research Laboratory of Electronics, M. I. T., January 15, 1964, p. 8.

2. S. G. Kukolich, Quarterly Progress Report No. 73, Research Laboratory of Electronics, M. I. T., April 15, 1964, p. 1.

3. S. G. Kukolich, Quarterly Progress Report No. 74, Research Laboratory of Electronics, M. I. T., July 15, 1964, p. 4.

4. R. S. Badessa, V. J. Bates, and C. L. Searle, Quarterly Progress Report No. 74, Research Laboratory of Electronics, M. I. T., July 15, 1964, p. 1.

5. R. P. Feynman, F. L. Vernon and R. W. Hellwarth, J. Appl. Phys. 28, 49 (1957).

6. A. Abragam, The Principles of Nuclear Magnetism (Oxford University Press, London, 1961), Chap. 2.

7. N. F. Ramsey, Recent Research in Molecular Beams, edited by I. Estermann (Academic Press, New York, 1959), Chap. 6.

8. N. F. Ramsey, Molecular Beams (Oxford University Press, London, 1956), Chap. 5.

B. NEUTRALITY OF ATOMS

Much data have accumulated from a gas efflux apparatus similar to that of Piccard and Kessler,[1] but with automatic volume changing to make it possible to isolate purely pressure-dependent effects. Figure I-2 is a schematic drawing of the apparatus. An electrometer measures the signal produced by gas escaping from an insulated container through an internal coaxial capacitor or deionizer. A computer program is being prepared to analyze the data by comparing the electrometer signal, after removing linear drift, with the suitably processed gas pressure DVM record. The calibrations that simulate the expected signal, and the noise figure of each efflux will be used to form a weighted average that, we hope, will reduce the standard deviations.
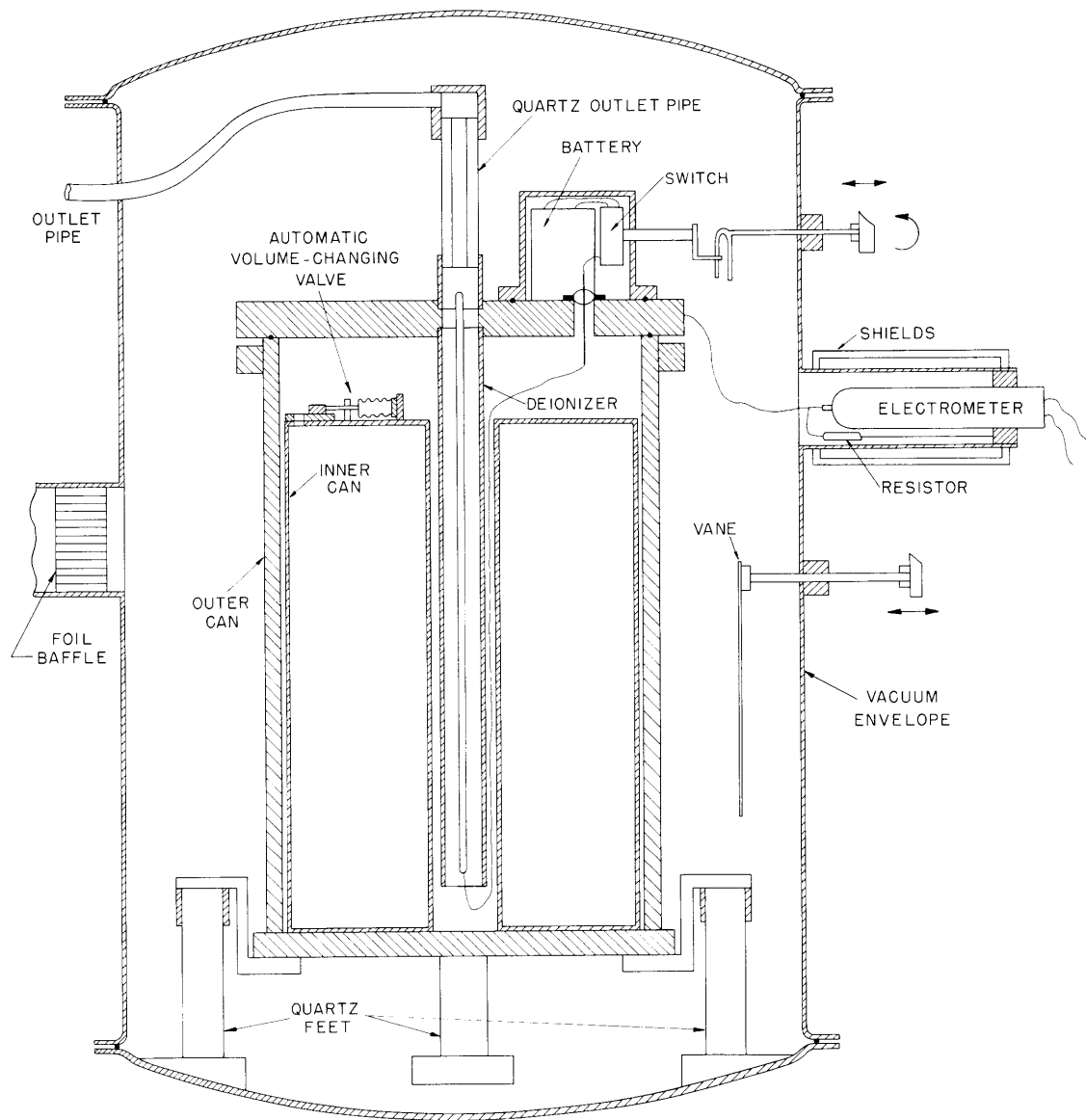
Fig. I-2. Cross section of the gas efflux apparatus.

Table I-1. Preliminary results of neutrality experiment.

Gas	Number of Effluxes	Deionizer Polarity	Effect*
H_2	24	+	$(1.0 \pm 0.8) \times 10^{-20}$
H_2	36	−	$(0.3 \pm 1.8) \times 10^{-20}$
D_2	24	+	$(1.5 \pm 0.6) \times 10^{-20}$
D_2	24	−	$(0.2 \pm 0.3) \times 10^{-20}$
He	60	+	$(3.2 \pm 0.4) \times 10^{-20}$
He	60	−	$(2.6 \pm 1.9) \times 10^{-20}$

*Interpreted as fundamental charges per molecule (molecules appear positive)

The results presented in Table I-1 are to be regarded as preliminary, in that they come from a simple analysis of approximately one-eighth of the data. The DVM records of groups of 6 effluxes were averaged and squares were counted under the resulting average curves to determine the amount of charge apparently carried by the gas. The standard deviations fluctuate on account of occasional large disturbances. The electrometer connected to the can, but with no gas flowing, has a noise equivalent input approximately $3 \times$ Johnson noise, or $\pm 6 \times 10^{-21}$, when interpreted as in Table I-1.

The data in Table I-1 form a block in which He was continually re-run to test whether or not the apparatus was changing its properties. The early He runs and the late ones, after H_2 and D_2 had been run, agree. Data taken before and after that of Table I-1 will be analyzed when the program has been prepared. There are data on the velocity dependence of the He signal, the effect of different kinds of filtering and gas purification, runs with no gas and with deionizer nominally at 0 volt, runs with gas recirculating equipment in operation and with none, runs with A, N_2, O_2, CO_2, and SF_6. An inspection of the A, N_2, O_2, and SF_6 data suggests that neither the signal nor the noise is significantly greater than that produced by H_2. CO_2 gives a very large signal (10^{-19}), leaving the apparatus negative, which is qualitatively similar to the situation observed earlier this year when gases that contained pump oil were used before the installation of N_2-cooled traps. Such data exhibit a marked asymmetry with respect to deionizer polarity, the large negative signals (positive charge leaving) being observed when the deionizer is positive, and less or none when it is negative.

These results, as well as that in He, are not now fully understood. Our plan is: (i) to study the outcome of more and better data analyses; (ii) to consider a few

Table I-2. Summary of results of various neutrality experiments.

Method	Gas	Effect[*]	Investigators
Gas	CO_2	$< 2.2 \times 10^{-19}$	Piccard and Kessler[1]
	A	$(4 \pm 4) \times 10^{-20}$	Hillas and Cranshaw[2]
	N_2	$(6 \pm 6) \times 10^{-20}$	Hillas and Cranshaw[2]
	H_2	$(-2.5 \pm 1.5) \times 10^{-20}$	King[3]
Efflux	He	$(4 \pm 2) \times 10^{-20}$	King[3]
	$CHCl_3$	$< 1.1 \times 10^{-16}$	Zorn[4]
Molecular	CsI	$< 4 \times 10^{-13}$	Hughes[5]
	Free Neutron	6×10^{-12}	Shapiro and Estulin[6]
	CsF	$< 2 \times 10^{-14}$	Zorn, Chamberlain, and Hughes[7]
Beam	KF	$< 1 \times 10^{-13}$	Zorn, Chamberlain, and Hughes[7]
	H_2	$< 2 \times 10^{-15}$	Zorn, Chamberlain, and Hughes[8]
	D_2	$< 2.8 \times 10^{-15}$	Zorn, Chamberlain, and Hughes[8]
Deflection	K	$(3.8 \pm 11.8) \times 10^{-17}$	Zorn, Chamberlain, and Hughes[8]
	Cs	$(1.3 \pm 5.6) \times 10^{-17}$	Zorn, Chamberlain, and Hughes[8]

[*]Interpreted as positive fundamental charge per molecule

[1] A. Piccard and E. Kessler, Arch. Sci. Phys. et Nat. (Geneva) 7, 340 (1925).

[2] A. M. Hillas and T. E. Cranshaw, Nature 184, 892 (1959); 186; 459 (1960).

[3] J. G. King, Phys. Rev. Letters 5, 562 (1960).

[4] J. C. Zorn, Limit for the Electron-Proton Charge Difference from a Vapor Efflux Experiment (H. M. Randall Laboratory of Physics, University of Michigan, 1964) (unpublished).

[5] V. W. Hughes, Phys. Rev. 76, 474 (1949) (A); 105, 170 (1957).

[6] I. S. Shapiro and I. V. Estulin, Zh. Eksperim. i. Teor. Fix. 30, 579 (1956). Translation: Soviet Phys. — JETP 3, 626 (1957).

[7] J. C. Zorn, G. E. Chamberlain, and V. W. Hughes, Bull. Am. Phys. Soc. 5, 36 (1960).

[8] J. C. Zorn, G. E. Chamberlain, and V. W. Hughes, Phys. Rev. 129, 2566 (1963).

additional experiments with this or similar apparatus, unsatisfactory as they are likely to be on account of the difficulty of knowing what is going on; and (iii) after a reasonable period of thought and discussion, to design and construct a beam-deflection experiment for He, H, etc., which now appears feasible with techniques developed in our laboratory for other investigations.

In conclusion, using D_2 and H_2 only we have, with a straightforward average:

$$+0.7 \pm 1.0 \times 10^{-20} \text{ fundamental charge/molecule.}$$

Averaging in He we have

$$+1.9 \pm 1.1 \times 10^{-20} \text{ fundamental charge/molecule.}$$

If it were premissible to divide the experimental upper limit on the charge per molecule by the number of nucleons in the molecule to obtain a charge per proton-electron pair or per neutron, the result for SF_6 would be $\sim 10^{-22}$ fundamental charge/p-e, n.

Table I-2 summarizes the results obtained by various investigators from similar experiments. Note that the newer He data agree (within error) with those from experiments with an apparatus published previously by the author which was different in detail. The standard deviation of the early H_2 data would have to be increased by 50 per cent to bring it into the range of the new results.

<div align="right">J. G. King</div>

<div align="center">References</div>

1. A. Piccard and E. Kessler, Arch. Sci. Phys. et Nat. (Geneva) 7, 340 (1925).

C. LOW-TEMPERATURE HELIUM BEAM EXPERIMENT

Construction of an atomic beam apparatus containing an He^4 source that can be operated from 300 °K to 0.5 °K is now substantially finished. Immediate plans for operation include measurement of intensity fluctuations and velocity distribution in beams of warm and cold He^4. One anticipates normal shot noise and a Maxwell-Boltzmann velocity distribution characteristic of the source temperature, with quantum effects probably remaining negligible at the lowest temperature, but such experiments, which should make future work with beams of slow He atoms feasible, have not been performed previously.

The mechanical aspect of this apparatus is shown in Fig. I-3. The high-vacuum system for the detector chamber reaches a base pressure of 3×10^{-10} Torr. Bakeout is not ordinarily required, provided that the chamber is released with argon before opening.

The untrapped 2-inch diffusion pump produces a 10^{-6} Torr vacuum at the site of the
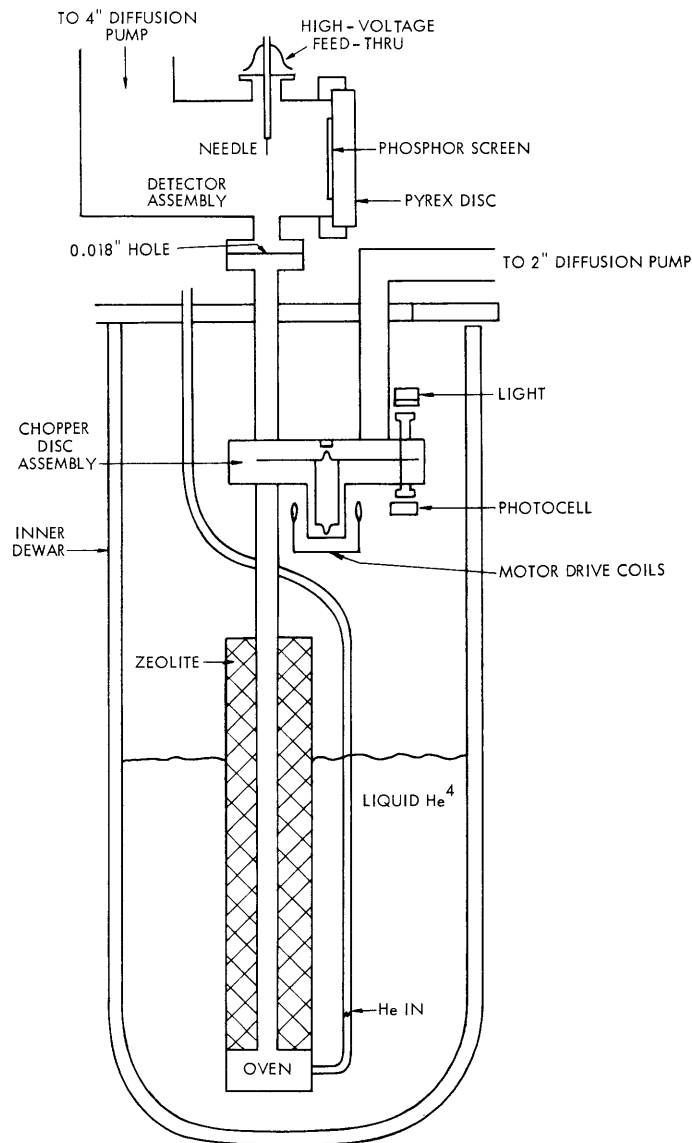
Fig. I-3.   Schematic drawing of the apparatus.

beam chopper with the Zeolite sorption pump at room temperature.   Adding liquid N_2 to the inner dewar reduces this pressure to the low 10^{-7} Torr range.

At present, work is directed toward making the detector scheme work.   Earlier work in this laboratory with field ionization needles has been in the medium high-vacuum range with poorly collimated beams.[1]   Atoms in the vicinity of the needle tip are ionized by the high electric field there ($\sim 5 \times 10^8$ volts/cm), and the ions strike a phosphor (P-16) screen which is viewed by a high-gain photomultiplier tube outside the vacuum envelope.   Aside from the 'internal' dark current noise in the photomultiplier, there are the following nonpressure-dependent components from the phosphor screen:

(i)   residual phosphor afterglow from previous excitation;

(ii) phosphor excitation by cosmic rays and residual alpha activity in the apparatus structure; and

(iii) DC field excitation of the phosphor (electroluminescence).

Component (iii) is worst at present, giving rise to a noise level 100 to 1000 times greater than the expected ion-luminescence signal. Efforts are being made to reduce or eliminate this by lowering the surface field at the phosphor by means of shield-grid arrangements. Investigation has shown that the electroluminescence is not due to ripple (RF or 60-cycle) in the high-voltage supply. Also, the electroluminescent intensity is exponentially dependent on needle potential, whereas for field ion-luminescence the intensity should be quadratic, with tip potential above a threshold at 10-15 kv.

<div align="right">W. D. Johnston, Jr.</div>

<div align="center">References</div>

1. T. L. Hawk and J. F. Prather, Application of Field Ionization to Molecular Beam Detection, S. B. Thesis, Department of Physics, Massachusetts Institute of Technology, June 1964 (unpublished).

D. CESIUM BEAM TUBE INVESTIGATION

Measurements have been made on the two cesium clocks to determine the cause of what appears to be a dependence of the offset upon temperature. Although the effect of temperature appeared to be unimportant in measurements made earlier in the year, more recent data indicate that the effect may have appeared small because the variation is nonlinear. At 21°C, for example, the effect of temperature upon the offset between clocks averaged 5 parts in 10^{12} per degree Centigrade, while at 27°C it dropped to one part in 10^{12} per degree Centigrade. At still higher temperatures the effect was not measurable. The cause of this temperature dependence is still not known. Although a drift in the loop electronics with temperature could account for some drift in frequency, drifts as large as one part in 10^{11} are hardly possible. To see if the temperature is somehow affecting the magnetic properties of the shields surrounding the beam tubes, we increased the strength of the C field by a factor of two. No corresponding change in the temperature effect occurred.

To study this temperature dependence in more detail, data are now being taken with one clock kept at a fixed temperature while the temperature of the other is varied over a wide range.

<div align="right">R. S. Badessa</div>

E. COMPUTER-AIDED CALCULATION OF FREQUENCY STABILITY

D. A. Brown derived an expression relating the variance of the frequency to the auto-correlation of the random part of the phase difference between two oscillators.[1] If θ(t),

the random part of the phase, is stationary, then we can make the identification

$$\sigma^2_{f\ avg\ T_o} = \left(\frac{1}{2\pi}\right)^2 \frac{2}{T_o^2} [\phi_{11}(0) - \phi_{11}(T_o)],$$ (1)

where $\phi_{11}(0)$ is the autocorrelation of the <u>random part of the phase</u> for zero delay [that is, the mean square of $\theta(t)$], and $\phi_{11}(T_o)$ is the autocorrelation of the <u>random</u> part of the phase for delay T_o. Thus the variance of the frequency as a function of averaging time T_o can be found very easily from the autocorrelation of the <u>random</u> part of the phase. This simple equation provides the direct link between various methods of data reduction, as shown in Fig. I-4.

A computer can be readily programmed to form $\phi_{11}(\tau)$, the autocorrelation function of the phase. As shown in Fig. I-4, it is now a simple matter to find the variance of
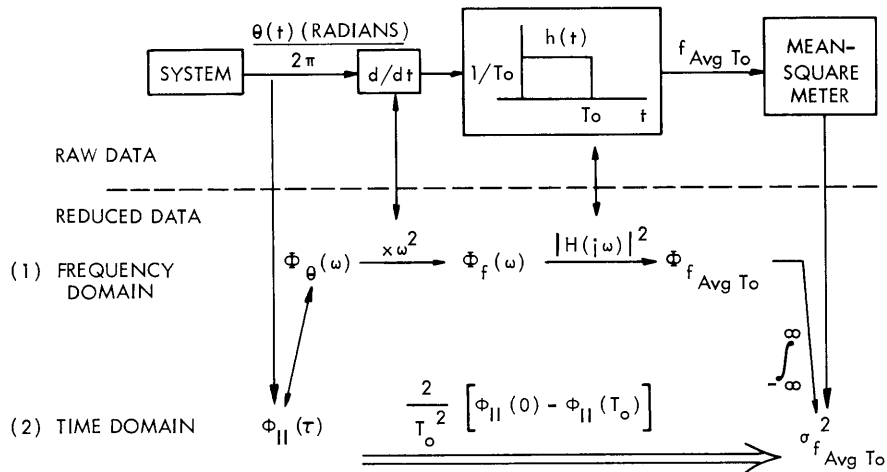

Fig. I-4. Summary of methods of data analysis.

frequency by using Eq. 1. With equal ease we can calculate the power spectrum of phase or the power spectrum of the frequency. As a specific example of this method, we have calculated $\phi_{11}(\tau)$, $\Phi_\theta(\omega)$, and $\sigma^2_{f\ avg\ T_o}$ for two oscillators on our PDP-1 computer. To avoid the phase ambiguities usually present in a phase detector, we used in our detection system two synchronous detectors that form $\sin\theta$ and $\cos\theta$. These signals were then fed to the PDP-1. The computer was programmed to find $\theta(t)$ from $\sin\theta$ and $\cos\theta$. It then removed the ramp of phase by a least-mean-square fit, then calculated $\phi_{11}(\tau)$ and its Fourier transform $\Phi_\theta(\omega)$, and the variance. These analysis methods will now be extended to include nonstationary phase functions.

R. D. Posner, C. L. Searle

References

1. D. A. Brown, Statistical Measurement of Frequency Stability, S. M. Thesis, Department of Electrical Engineering, M. I. T. , August 1962.

F. VELOCITY OF LIGHT

The mechanical design of our apparatus has been considerably modified to reduce vibration problems. Specifically, many of the optical mounts have been rebuilt, and the piston support has been completely redesigned so that all mechanical motion is with reference to the main base plate of the apparatus. These changes have reduced by at least an order of magnitude the susceptibility of the apparatus to shock and vibration.

An accurate measurement of the diameter and ellipticity of the quartz cavity has been made. The diameter was measured by means of a Cleveland Indi-ac electronic indicator and a set of Johanson gauge blocks. Measurements were made at three points in the cavity. The results are summarized in Table I-3.

Table I-3. Diameter.

Location of Measurement	Result (inches)
1/2 inch from marked end	6. 3461
Center	6. 34615
1/2 inch from unmarked end	6. 3461

The estimated error in each of these measurements is $\pm 5 \times 10^{-5}$ inch.

The ellipticity of the cylinder was measured on a Taly-rond. The results are given in Table I-4.

Table I-4. Ellipticity.

Location of Measurement	Value of Ellipticity (inches)
1/2 inch from marked end	8×10^{-6}
4 5/8 inches from marked end	5×10^{-6}
4 5/8 inches from unmarked end	5×10^{-6}
1/2 inch from unmarked end	5×10^{-6}

The accuracy of these measurements is $\pm 3 \times 10^{-6}$ inch.

These measurements give the diameter to better than one part in 10^5. Because the diameter is suppressed by a factor of 16 in our experiment, these measurements can be used to obtain a measurement of the velocity of light that is accurate within approximately 5 parts in 10^7.

M. A. Yaffee, C. L. Searle